

# Effect of Laser Dimple Texturing on Aspect Ratio and Heat Affected Zone of Copper Thin Foils

Gourav Vivek Kulkarni<sup>1</sup>, Bharatish A<sup>1\*</sup>, Kaushal Rao B S<sup>1</sup>,  
Manojkumar Y N<sup>1</sup>, Manjunatha B L<sup>1</sup>, Dharanish D<sup>1</sup>, Gagan C<sup>1</sup>

<sup>1</sup> Department of Mechanical Engineering, RV College of Engineering, Bengaluru

## Abstract

In industrial settings, the demand for precision marking techniques is critical for applications like thin foil drilling, perforation, tagging, and texturing. Laser ablation has emerged as a versatile and accurate method for meeting these precision requirements. Notably, the use of copper thin foils as seed layers for semiconductors, electronic component coatings, and heat sinks in electronics has gained prominence. However, the literature has shown a scarcity of studies addressing laser ablation in this context. This study delves into laser ablation processes, specifically targeting dimple formation on a 100-micron-thick copper foil. To systematically explore the impact of laser parameters, such as power, scanning speed, and pulse frequency, a Taguchi L27 experimental design was employed. Two key response variables were investigated: the dimple aspect ratio, providing insight into geometric characteristics, and the heat-affected zone, which represents the surface response. Through the application of response surface methodology (RSM), the study identifies optimal parameter values: a power level of 27.76%, a scanning speed of 100 mm/s, and a pulse frequency of 15 kHz. These optimized settings aim to achieve two primary objectives: bringing the dimple aspect ratio closer to unity, indicating a more desirable shape, and minimizing the extent of the heat-affected zone. This research contributes valuable insights into enhancing precision in laser ablation processes for applications involving copper foils in industrial contexts.

**Keywords:** Ablation, laser, copper, foil, dimple

## 1.0 Introduction

Laser ablation refers to the process of removal of material from the surface of a solid by irradiating it with a laser beam thus forming typical patterns that include dimples, grooves and other free forms. Micropatterns are

---

\*Mail address: Bharatish A, Assistant Professor, Department of Mechanical Engineering, RV College of Engineering, Bengaluru – 59  
Email: bharatisha@rvce.edu.in, Ph: 9886445035

created on a surface by a laser beam in which the laser generates a controlled amount of energy at a specific location on the surface causing localized melting or ablation. Tribological components use this to reduce friction and wear between moving parts, bonding between two surfaces can be improved in case of adhesive applications. It is considered an advantageous process as it has high precision, the process is contactless and the patterns can be customized to the requirements. The process applies to a large variety of materials like metals, polymers, ceramics, composites etc. Marking of patterns on intricate surfaces can be easily facilitated by this technique. Some of the limitations include need for process optimization of the laser parameters and the scanning patterns and the consistency owing to other factors like surrounding environment.

Kleefoot et al. [1] investigated parameter dependency of perforation using ultra shot laser pulses on a copper foil used for electrodes. The factors considered were pulse duration, number of pulses and single pulse energy to determine the ablation depth. It was found that moderate fluences and low number of pulses, the depth of hole can be linearly increased by increasing the number of pulses per hole. Moze et al [2] studied textured copper surfaces with nanosecond laser and considered scanning speed, frequency and pulse length as the parameters. The responses were textures and their effects on the enhancement of the critical heat flux and heat transfer coefficient.

Samanta et al. [3] studied the wettability of a surface considering the parameters such as pulse energy, repetition rate, scanning speed, processing environment and polarization. It was found that size and shape of the texture is controlled by varying the parameters like scanning speed and spot size. Cheng et al. [4] studied the wettability properties of coated copper surfaces that were textured with picosecond laser. Parameters considered were scribing speed, repetition rate, hatch spacing and focus diameter and their effects on responses such as surface roughness and chemical transitions were found and conclusions regarding the hydrophilicity were drawn. Allahyari et al. [5] studied the laser surface texturing of copper and the variation in wetting response with the pulse fluence in which it was found that hydrophobic surfaces could be formed with controlled.

From the review of literature, it was found that the laser ablation studies on copper thin foils have been scarcely reported. The aspect ratio and heat affected zone are some of the critical responses which needs to be optimized for improving the laser ablation quality. Hence this paper focuses on optimizing the laser parameters for minimizing the heat

affected zone and improve the aspect ratio simultaneously using response surface methodology.

## 2.0 Experimental Setup

A Laser Marking Machine with Transverse Electromagnetic Beam Mode was used. The machine has a nominal average power of 20 W, pulse frequency of 20-100 kHz, pulse width of 100 ns and rated wavelength of 1064 nm. Software used was EZCad. A LAGEN optical microscope with 10X magnification was used to obtain the results. Software used was ISC Capture.

## 3.0 Experimental Procedure

An L27 Taguchi array was considered for the factors such as power measured in percentage maximum power (20 W), scanning speed in mm/s and pulse Frequency in kHz [2,3,4]. The responses considered were aspect ratio with nominal the best condition [6,7] and heat affected zone with smaller the better condition [8,9]. Three holes were marked for every combination of the factors thus summing up to 81 holes. Table 1 provides the summary of factors and responses recorded.

**Table 1.** L27 Taguchi array for factors and responses of ablation

Sl. No	Power (%)	Speed (mm/s)	Frequency (kHz)	Aspect Ratio			Heat Affected Zone		
				Hole 1	Hole 2	Hole 3	Hole 1	Hole 2	Hole 3
1	25	100	15	0.997	0.988	0.998	36.07	38.49	39.26
2	25	100	15	0.977	0.996	0.999	42.21	33.96	41.19
3	25	100	15	0.996	0.983	0.987	43.88	38.69	34.52
4	25	150	20	0.980	0.987	0.985	37.18	41.05	40.31
5	25	150	20	0.994	0.973	0.985	42.79	41.43	40.20
6	25	150	20	0.970	0.983	0.973	42.00	37.60	41.05
7	25	200	25	0.965	0.983	0.979	45.01	43.44	41.35
8	25	200	25	0.994	0.984	0.999	37.07	48.23	33.10
9	25	200	25	0.985	0.981	0.984	44.34	35.58	32.31
10	30	100	20	0.983	0.990	0.975	36.57	35.51	32.32
11	30	100	20	0.983	0.998	0.974	31.79	35.35	33.57
12	30	100	20	0.986	0.983	0.993	42.43	39.06	32.21
13	30	150	25	0.988	0.985	0.967	38.30	49.96	52.34
14	30	150	25	0.996	0.991	0.983	40.50	44.53	47.13
15	30	150	25	0.997	0.993	0.999	47.90	39.72	46.53

Sl. No	Power (%)	Speed (mm/s)	Frequency (kHz)	Aspect Ratio			Heat Affected Zone		
				Hole 1	Hole 2	Hole 3	Hole 1	Hole 2	Hole 3
16	30	200	15	0.985	0.988	0.988	51.11	50.93	51.82
17	30	200	15	0.997	0.998	0.991	50.83	54.02	48.39
18	30	200	15	0.991	0.994	0.991	47.52	46.63	49.39
19	35	100	25	0.974	0.967	0.971	32.51	36.56	39.80
20	35	100	25	0.997	0.987	0.992	43.05	49.45	37.44
21	35	100	25	0.994	0.992	0.997	41.79	42.38	37.04
22	35	150	15	0.995	0.989	0.990	28.52	53.52	65.13
23	35	150	15	0.999	0.999	0.998	61.46	40.94	52.58
24	35	150	15	0.989	0.979	0.988	49.23	53.69	51.90
25	35	200	20	0.985	0.984	0.997	49.79	36.54	49.45
26	35	200	20	0.990	0.989	0.996	43.57	49.58	54.42
27	35	200	20	0.999	0.993	0.999	45.04	49.88	51.01

## 4.0 Results and Discussions

### 4.1 Effect of laser parameters on aspect ratio

From the main effects plot for means as shown in Fig 1, it can be observed that as the Power is increased between the levels, the aspect ratio value also increases and tends to unity, which is the requirement. With respect to Scanning speed, from 100 mm/s to 150 mm/s, the aspect ratio is seen to decrease but with further increase in the scanning, speed to 200 mm/s, the mean aspect ratio also increases significantly. There is a pronounced decrease in the aspect ratio with the increase in the frequency values from 15 kHz to 20 kHz and with further increase, there is no significant reduction observed.

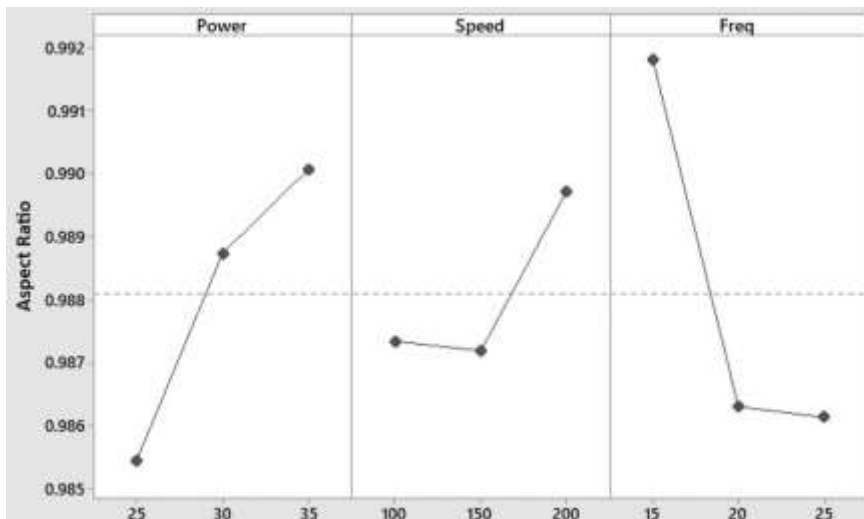


Fig. 1. Main effects plot for Mean of Means for Aspect Ratio

It can be observed in Fig 2 from the main effects plot considering the SN ratios that for the Power, the maximum is at 30% while for the scanning speed, it is at 200 mm/s and for the frequency, it is at 15 kHz. As the power increases, the SN ratio increases and decreases with further increase in the power. In case of the scanning speed, it shows an increasing trend throughout and the trend is observed to be decreasing in case of the increase in factor values of Frequency. Thus, for the optimisation of the aspect ratio considering the mean effects plot, the levels of the factors should be 30% power, 200 mm/s scanning speed and 15 kHz of frequency.

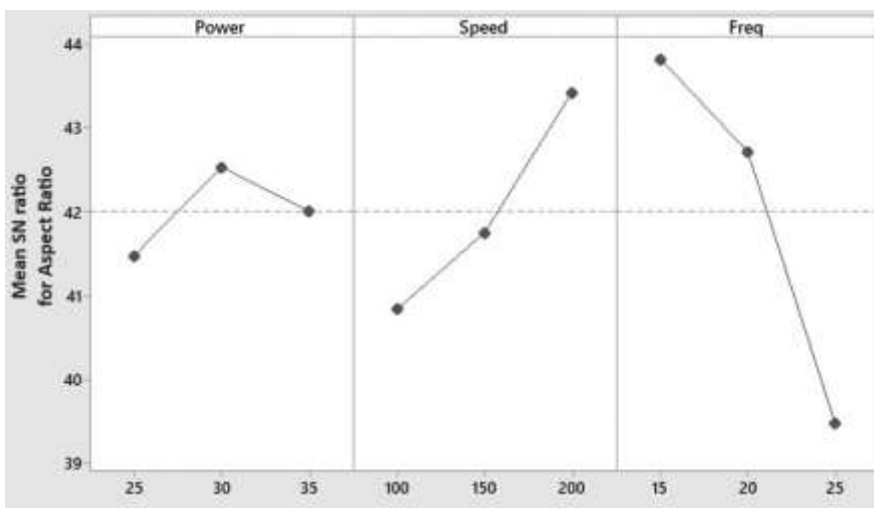


Fig. 2. Main effects plot for Mean of SN Ratios for Aspect Ratio

## 4.2 Effect of laser parameters on heat affected zone

From the main effects plot as shown in Fig. 3, it can be observed that as the power increases from 25% to 35%, there is a significant increase in the heat affected zone which can be attributed to discharge of increasing energy [10]. With regards to the increase in scanning speed, it is observed that between 100 mm/s and 150 mm/s there is a significant increase in the heat affected zone, which is not that significant for a further increase, which is on account of the lesser dwelling of the pulses at a point [11]. With increase in frequency, the heat affected zone initially decreases but gradually increases with further increase in the frequency. This can be attributed to the effectiveness of the ablation taking place on the copper foil [12].

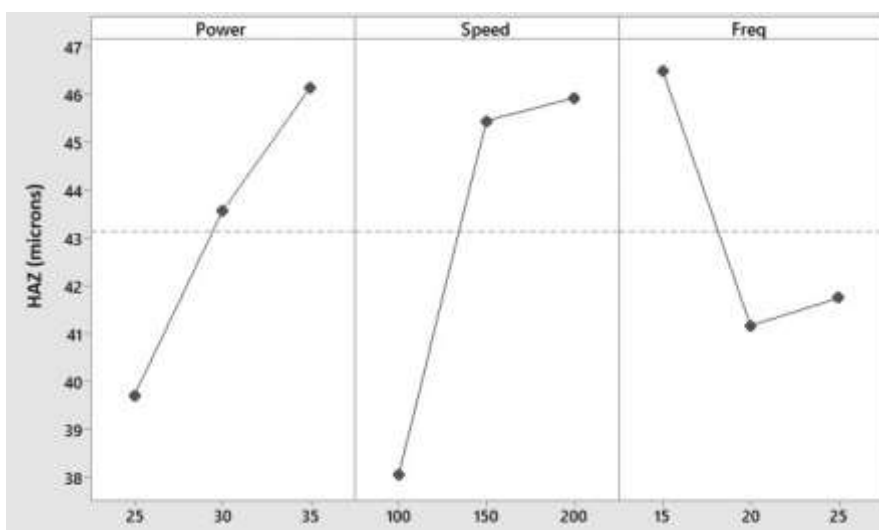


Fig. 3. Main effects plot for Mean of Means for Heat Affected Zone

The Signal to Noise Ratio Plots in Fig 4 show that with an initial increase in the power, there is slight increase in the ratio, which further decreases significantly as the power increases further. As with the scanning speed, there is no significant increase in the ratio up to 150 mm/s but on further increase, the ratio increases significantly. The trend as observed for frequency is such that up to 20 kHz, the ratio increases and thereafter decreases significantly. Thus, for the consideration of optimal values for heat affected zone as per the desired results, power can be 30%, scanning speed shall be 200 mm/s and the frequency shall be 20 kHz.

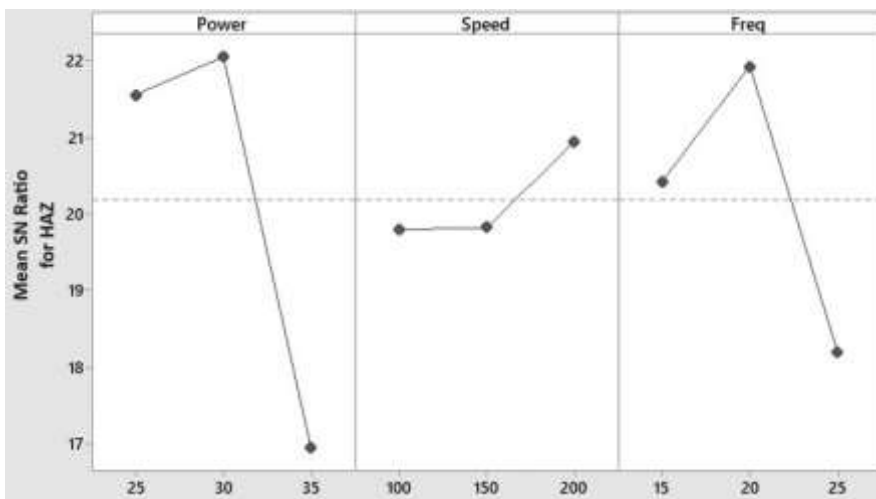


Fig. 4. Main effects plot for Mean of SN Ratios for Heat Affected Zone

### 4.3 Response Surface Regression models

The Response Surface Regression equation correlating the aspect ratio with the factors such as power, scanning speed and frequency is as follows.

$$\text{Aspect Ratio} = 0.9820 + 0.000462(P) + 0.000024(S) - 0.000568(F) \quad (1)$$

Where P is the laser power (%), S is scanning speed (mm/s), F is Frequency (kHz)

The R<sup>2</sup> value for the above correlation was found to be 61.17%. The Pareto chart in Fig 5 shows that the factor having the most significant effect on the aspect ratio is the frequency of pulse. This can be attributed to the quantum of pulses incident on a particular surface in a given time. The scanning speed is seen to be the least significant.

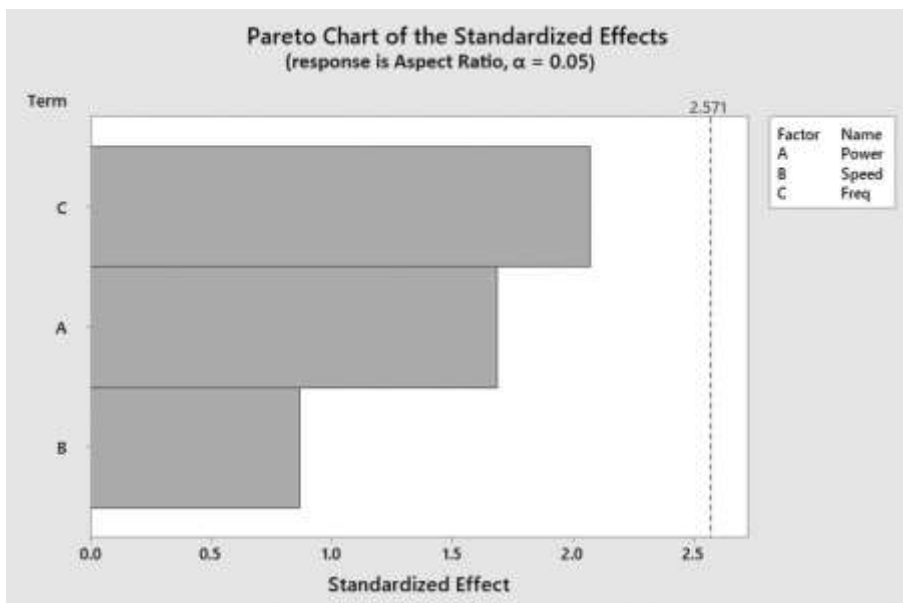


Fig. 5. Pareto Chart for Standardized effects for mean aspect ratio

The Response Surface Regression equation correlating the heat affected zone with the factors such as power, scanning speed and frequency is as follows:

$$\begin{aligned} \text{Heat Affected Zone} \\ = 21.49 + 0.644(P) + 0.0790(S) - 0.476(F) \quad (2) \end{aligned}$$

Where P is the laser power (%), S is scanning speed (mm/s), F is Frequency (kHz)

The  $R^2$  value for the above correlation was found to be 79.90%. The Pareto chart in Fig 6 shows that the factor having the most significant effect on the heat affected zone is the scanning speed of pulse. This can be attributed to the fact that at the circumference, owing to the pattern of ablation, the beam reverses its direction in quick succession, leaving a certain additional energy of ablation. The frequency is seen to be the least significant.



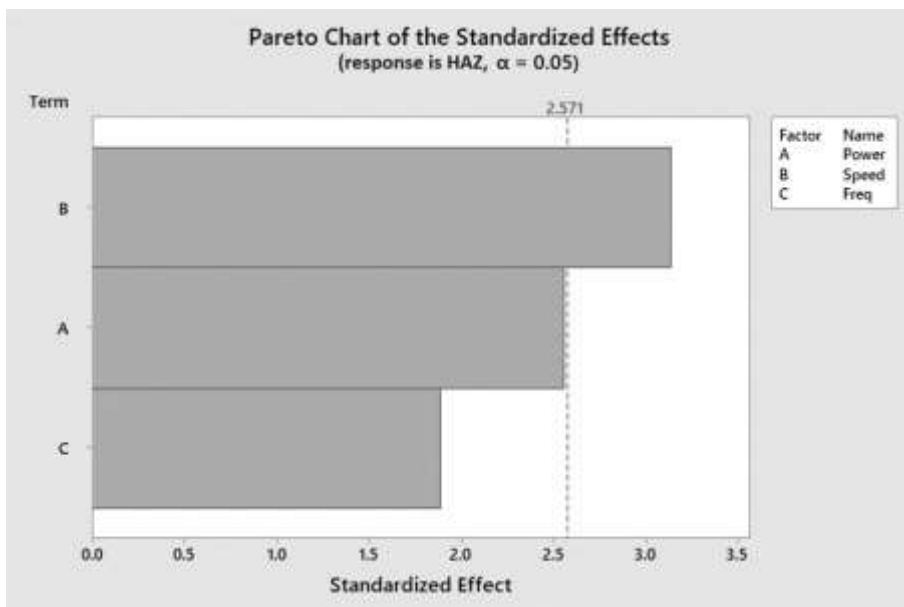


Fig. 6. Pareto Chart for Standardized effects for mean Heat Affected Zone

The residual plots are as shown in Fig 7 and 8 for mean aspect ratio and heat affected zone. The normal Probability plots show that except two points, the others follow the trend line. The Histograms are skewed to the right indicating a deviation from the mean. The Normal Probability plots showed a nearly evenly distribution of points about the trend line except two. The histogram is also nearly symmetric.

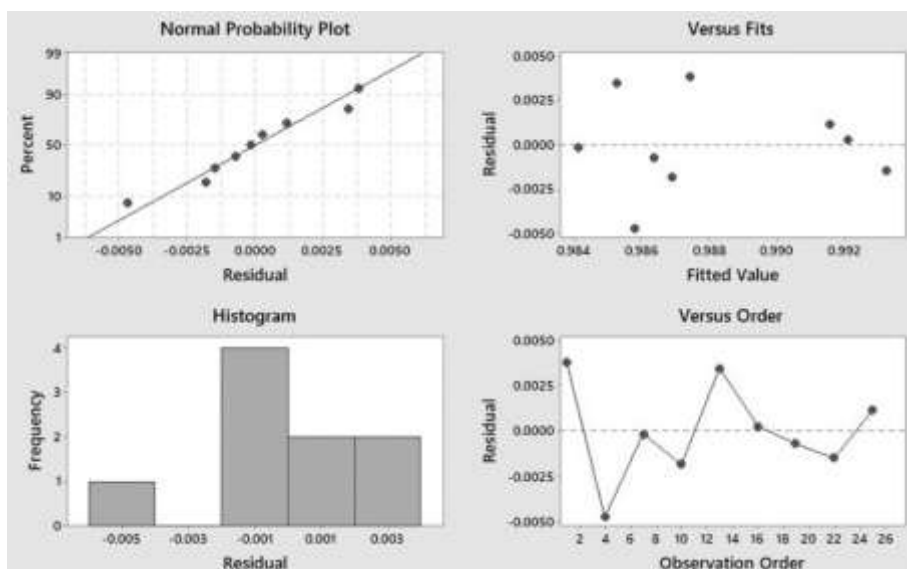


Fig. 7. Residual Plots for Mean Aspect Ratio

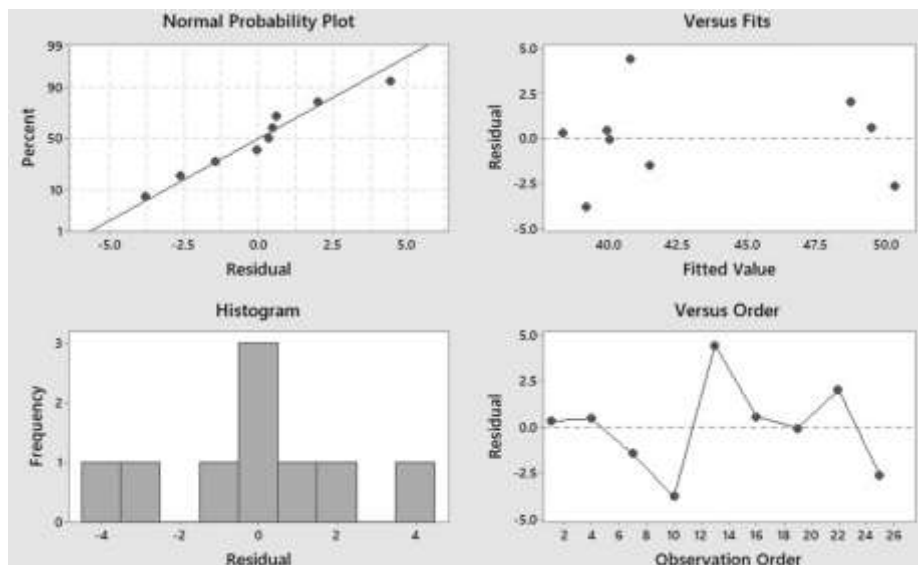


Fig. 8. Residual Plots for Mean Heat Affected Zone

#### 4.4 Optimization of laser parameters using Response Surface Methodology

This test provides the optimal values of the factors that can yield the optimized conditions as per the given inputs. From the previous studies it was found that certain specified levels of the factors are optimum for the individual responses. However for the experiment as a whole, it is essential to obtain a complete response optimization to best fit the model as per the experimental results.

It can be observed from Fig. 9 that for the given optimum conditions that the aspect ratio shall be nearer to unity and the heat affected zone shall be minimum, the factor level value for power shall be 27.7666% i.e., 5.55332 W, speed shall be 100 mm/s and the frequency shall be 15 kHz. These values are for the considered intervals of the levels for the different factors and can be refined by further experimentation either by increment or decrement in the same.

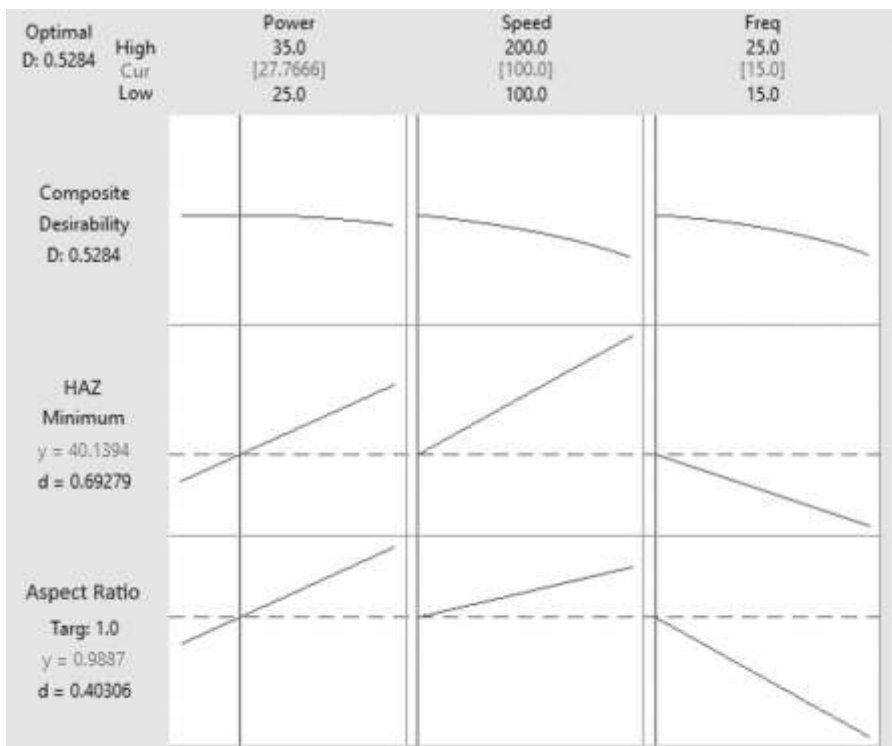


Fig. 9. Response optimization for means

## 5.0 Conclusion

In conclusion, our study reveals valuable insights into the critical factors influencing laser ablation processes on thin copper foils. We have identified that the aspect ratio of the dimples, a crucial geometric characteristic, is primarily influenced by variations in pulse frequency and power. Conversely, the size of the heat-affected zone, an essential consideration for material integrity, is predominantly affected by changes in scanning speed and power.

Through the application of response surface methodology (RSM), we have successfully determined the optimal parameter values for achieving our desired outcomes. To attain an aspect ratio approaching unity and minimize the heat-affected zone, the optimal combination of parameters is as follows: 27.76% power, 100 mm/s scanning speed, and 15 kHz pulse frequency.

It is important to acknowledge that while these results offer a promising foundation for precise laser ablation on thin copper foils, further refinement can be achieved through additional experimentation and in-

depth analysis. The complexity of industrial applications often requires continuous optimization to meet stringent standards of precision and quality. Therefore, this study serves as a valuable starting point for enhancing the precision and accuracy of laser ablation processes in a variety of industrial contexts involving copper foils.

## References

1. M.-J. Kleefoot, et al., "Investigation on the parameter dependency of the perforation process of graphite-based lithium-ion battery electrodes using ultrashort laser pulses," *Journal of Laser Applications*, 34(4), 2022.
2. M. Može, et al., "Nanosecond laser-textured copper surfaces hydrophobized with self-assembled monolayers for enhanced pool boiling heat transfer," *Nanomaterials*, 12(22), 4032, 2022.
3. A. Samanta, et al., "Roles of chemistry modification for laser textured metal alloys to achieve extreme surface wetting behaviors," *Materials & Design*, 192, 108744, 2020.
4. H.-C. Cheng, et al., "Roughness and wettability properties of plain and silica-coated copper surfaces textured with picosecond laser," *Applied Surface Science*, 514, 145918, 2020.
5. E. Allahyari, et al., "Laser surface texturing of copper and variation of the wetting response with the laser pulse fluence," *Applied Surface Science*, 470, 817-824, 2019.
6. M. Guillong, et al., "Evaluating the reliability of U–Pb laser ablation inductively coupled plasma mass spectrometry (LA-ICP-MS) carbonate geochronology: matrix issues and a potential calcite validation reference material," *Geochronology*, 2(1), 155-167, 2020.
7. D.-D. Nguyen, et al., "Seismic damage analysis of box metro tunnels accounting for aspect ratio and shear failure," *Applied Sciences*, 9(16), 3207, 2019.
8. Y. Zhang, et al., "Study on machining characteristics of magnetically controlled laser induced plasma micro-machining single-crystal silicon," *Journal of Advanced Research*, 30, 39-51, 2021.
9. M. Fikry, W. Tawfik, and M. M. Omar, "Investigation on the effects of laser parameters on the plasma profile of copper using picosecond laser induced plasma spectroscopy," *Optical and Quantum Electronics*, 52, 1-16, 2020.

10. J. Hijam, R. Balhara, and M. Vadali, "Investigating Double-Scan Strategies for Reducing Heat-Affected Zone in Laser Surface Melting," *Available at SSRN 4531337*.
11. S. Liu and M. Pan, "Research on a forward-looking scanning imaging algorithm for a high-speed radar platform," *IET Signal Processing*, 17(6), e12221, 2023.
12. T. Sonar, et al., "An overview of welding of Inconel 718 alloy-Effect of welding processes on microstructural evolution and mechanical properties of joints," *Materials Characterization*, 174, 110997, 2021.